

duty factor and average beam intensity compared with the electron ring accelerator with pulsed compression system. The axial injection is not restricted to one beam as is the case with radial injection in the median plane. Thus, the electron beams from two or more accelerators could be injected simultaneously to increase the number of electrons in the ring. Injection efficiency would be 100% as no electric inflector system restricts the motion of the beam. Iron could be used (e.g., in the return path of the magnetic flux) to reduce the power requirements.

With respect to the electron accelerator it appears that an improved version of the 20-MeV linac presently installed at Argonne National Laboratory could meet the requirements.

Finally, it should be noted that a combination of axial injection from a low-energy accelerator with subsequent pulsed compression might offer some advantages compared with the radial inflector system presently used.

Note added in proof. — After writing this paper

we have learned that N. C. Christofilos, Lawrence Radiation Laboratory, also proposed a method of static compression which is described in an unpublished internal report.

*Work supported in part by the U. S. Atomic Energy Commission.

¹V. I. Veksler, in Proceedings of the CERN Symposium on High-Energy Accelerators and Pion Physics, Geneva, Switzerland, 1956 (CERN Scientific Information Service, Geneva, Switzerland, 1956), p. 80.

²V. I. Veksler et al., in Proceedings of the Sixth International Conference on High Energy Accelerators, Cambridge, Massachusetts, September, 1967 (to be published), p. 289.

³Lawrence Radiation Laboratory Report No. UCRL-18103, 1968 (unpublished).

⁴The recent experiment by A. W. Trivelpiece and co-workers, who trapped a 0.5-MeV electron ring in a pulsed mirror field [Phys. Rev. Letters **21**, 1436 (1968)], represents a method of pulsed compression which may also be applicable to the electron ring accelerator.

WIDE-ANGLE BREMSSTRAHLUNG*

R. H. Siemann, W. W. Ash,† K. Berkelman, D. L. Hartill, C. A. Lichtenstein, and R. M. Littauer
Laboratory of Nuclear Studies, Cornell University, Ithaca, New York

(Received 22 January 1969)

We have measured the bremsstrahlung yield at 6.2° in the reaction $e^- + C \rightarrow e^- + C + \gamma$ using incident-electron energies up to 9.5 GeV. The data confirm the predictions of quantum electrodynamics for timelike electron four-momenta up to 1 GeV.

Although quantum electrodynamics has been checked experimentally for a number of high-energy electromagnetic processes,¹ it does not follow that the theory is necessarily valid. If the propagation or coupling of timelike virtual electrons of large four-momentum were somehow anomalous, none of the existing experiments would have detected it. However, in the electron bremsstrahlung process one of the two dominant amplitudes [Figs. 1(b) and 1(c)] involves a timelike² virtual electron,

$$q_t^2 = (p_2 + k)^2 > 0,$$

so that a measurement of the yield at large values of q_t^2 serves as a unique test of the validity of quantum electrodynamics.

In the laboratory frame,

$$q_t^2 = 4p_2 k \sin^2 \frac{1}{2} \theta_{\gamma 2},$$

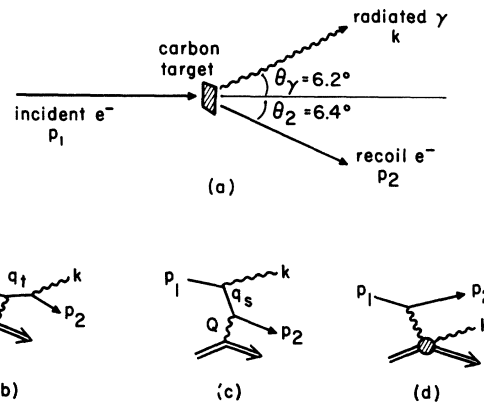


FIG. 1. (a) Schematic of the geometry of the experiment showing the momentum and angle definitions used in this paper. (b) and (c) Feynman diagrams for the Bethe-Heitler amplitudes in bremsstrahlung. (d) Diagram for the Compton amplitude.

neglecting the electron mass ($\theta_{\gamma 2}$ is the angle between the final electron and the radiated photon). The timelike electron is therefore far off the mass shell if the final energies and angles are large. In order to minimize the dependence of the yield on nuclear form factors, the momentum transfer Q to the nucleus should be kept low by requiring that the resultant transverse momentum of the final electron-photon system be zero.³

In the present experiment⁴ the circulating electron beam of the Cornell 10-GeV synchrotron struck a carbon target in a field-free straight section. Bremsstrahlung photons were observed at 6.2° in coincidence with the corresponding recoil electrons at 6.4° on the opposite side of the beam. The carbon nucleus recoiled with less than 85 MeV/c and was not observed. The final electrons were momentum analyzed by a pair of vertically focusing quadrupole magnets and detected in scintillators and a lead-glass Čerenkov shower counter. The momentum resolution $\Delta p_2/p_2$ was 7.5%. The photons were detected in a similar shower counter, with an energy resolution $\Delta k/k = 12\%$ (full width at half-maximum). Between the two electron quadrupoles was a lead plug which divided the aperture vertically into aperture 1 which was centered on the $\vec{p}_1 - \vec{k}$ plane and aperture 2 misaligned vertically by 3° .

For each $e\gamma$ coincidence the shower-counter pulse heights and the electron-photon time-of-flight difference were recorded. Except for random coincidence subtraction (less than 10%) no significant background appeared in these distributions. In fact, when the electron magnet current was mistuned so that $p_2 = \frac{1}{2}(p_1 - k)$, no real coincidences were observed.

The incident beam was monitored by observing the forward bremsstrahlung flux with a secondary-emission monitor behind a 3.2-cm lead converter, calibrated against a standard quantometer.⁵ This was further checked by measuring the elastic ep scattering rate from a polyethylene target using the same electron spectrometer and flux monitor. We believe the absolute normalization of our measured rates is good to 5%.

The detection geometry was kept fixed throughout the experiment. From 300 to 500 wide-angle bremsstrahlung events were observed at each of seven incident energies from $p_1 = 2.5$ to 9.5 GeV. The 8.75-GeV run was repeated with a copper target instead of carbon. The yield followed the expected Z^2 dependence.

The two Bethe-Heitler diagrams [Figs. 1(b) and 1(c)] account for most of the bremsstrahlung am-

plitude. The approximate cross section⁶ from these graphs is

$$\frac{d\sigma}{(dp_2/p_2)d\Omega_2 d\Omega_\gamma} \approx \frac{8Z^2\alpha^3}{\pi^2} \frac{p_2(p_1^2 + p_2^2)}{k p_1^4 \theta_2^2 \theta_\gamma^4 (\theta_2 + \theta_\gamma)^2} \frac{r^2}{(1+r^2)^2},$$

where $r = Q_\perp/Q_\parallel$ is the ratio of the components of the momentum transferred to the nucleus transverse and parallel to the beam direction. The longitudinal momentum transfer is given approximately by $Q_\parallel \approx \frac{1}{2} p_1 \theta_2 \theta_\gamma$, while Q_\perp depends sensitively on the final electron-photon transverse momentum balance. There is a sharp dip at $r = 0$, then a maximum at $r = 1$, and finally a decrease as r is increased further. Although aperture 1 was centered on $r = 0$, it was too broad to be sensitive to the dip but instead spanned the maximum out to $r \approx 1.4$. Aperture 2 was centered around $r \approx 4$ and gave a considerably reduced coincidence rate because of the r dependence of the Bethe-Heitler cross section and the effect of the nuclear form factor. Only data from aperture 1 were used in the test of quantum electrodynamics. Aperture 2 provided a check that the events detected were indeed coming from the wide-angle bremsstrahlung process.

The Bethe-Heitler cross section was multiplied by the square of the carbon form factor⁷ (a 28% effect in the worst case) and corrected for higher order radiative effects (10 to 14%), then Monte Carlo integrated over the experimental apertures⁸ to give a Bethe-Heitler yield prediction at each of the incident energies p_1 and for each of the two electron apertures. The ratio of aperture-1 yield to the corresponding Bethe-Heitler prediction is plotted in Fig. 2 as a function of the total invariant mass $M_{e\gamma}$ of the final electron-photon system:

$$M_{e\gamma} = [4p_2 k \sin^2 \frac{1}{2}(\theta_2 + \theta_\gamma)]^{1/2} = 0.110 p_1.$$

The four-momentum of the virtual electron in each of the Bethe-Heitler diagrams is given by $q_t^2 = M_{e\gamma}^2$ and $q_s^2 = -0.71 M_{e\gamma}^2$. Also plotted for a consistency check are the predicted and observed ratios of the aperture-2 and aperture-1 yields.

Another amplitude which contributes to wide-angle bremsstrahlung is the forward nuclear Compton scattering of the virtual photon [Fig. 1(d)]. The cross section for this process is estimated from the optical theorem and the total γ -

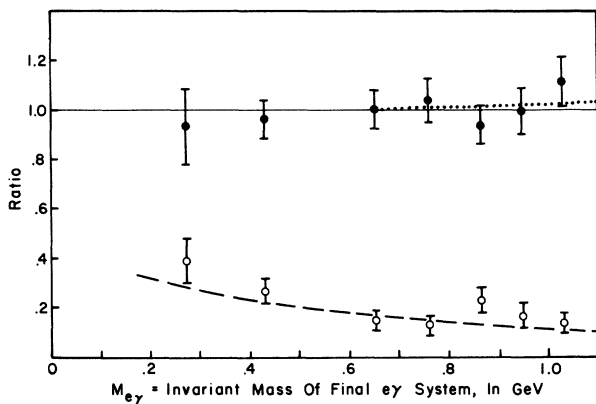


FIG. 2. Experimental results. The upper points are the ratio of the experimental aperture-1 yields to the corresponding Bethe-Heitler predicted yield. The estimated Compton correction to the predicted yield is shown in the dotted curve. The lower points and dashed curve give the measured and predicted ratios of aperture-2 and aperture-1 yields. The error limits include all experimental and theoretical uncertainties, except for the overall 5% uncertainty in beam monitoring.

nucleus cross section. The virtual photon is spacelike; so no special enhancement is expected off the mass shell. The estimate is less than 3% of the Bethe-Heitler cross section. The interference term is expected to be negligible because the Compton amplitude is almost purely imaginary. The net correction is plotted in Fig. 2.

A possible background of $e\gamma$ coincidences comes from the electroproduction of π^0 mesons decaying into photons, one of which is detected. The expected electroproduction yield is estimated from the well-known relation to photoproduction and turns out to be less than 1% of the wide-angle bremsstrahlung rate. This background is even further suppressed by the pulse-height requirement in the photon-shower counter.

The conclusion implied by Fig. 2 is that the aperture-1 data are in excellent agreement with the prediction of quantum electrodynamics, both in absolute magnitude and in energy dependence. No violation is seen to an accuracy of 10%, up to an effective mass of $M_{e\gamma} = 1030$ MeV. Since the theory has already been verified for spacelike electrons over this four-momentum range,¹ the present results now confirm it in the timelike region.⁹

For purposes of comparison with other experiments, we quote the 95% confidence upper limit on the slope of the experiment/theory ratio R ,

$$\Lambda^{-1} = \left[\frac{1}{2} \left(\frac{dR}{dM_{e\gamma}^2} \right) \right]^{1/2} < 9 \times 10^{-15} \text{ cm.}$$

We are indebted to A. Ramanauskas and E. C. Loh for valuable assistance.

*Work supported by the National Science Foundation.

†Present address: Palmer Physical Laboratory, Princeton University, Princeton, N. J.

¹We list here some of the more recent high-energy electrodynamic experiments: H. Alvensleben, U. Becker, W. K. Bertram, M. Binkley, K. Cohen, C. L. Jordan, T. M. Knasel, R. Marshall, D. J. Quinn, M. Rohde, G. H. Sanders, and S. C. C. Ting, Phys. Rev. Letters **21**, 1501 (1968) (spacelike electrons); J. K. dePagter, J. I. Friedman, G. Glass, R. C. Chase, M. Gettner, E. vonGoeler, R. Weinstein, and A. M. Boyarski, Phys. Rev. Letters **17**, 767 (1966), and in Proceedings of the Third International Symposium on Electron and Photon Interactions at High Energies, Stanford Linear Accelerator Center, 1967 (Clearing House of Federal Scientific and Technical Information, Washington, D. C., 1968), p.424 (spacelike muons); W. C. Barber, G. Gittelmann, G. K. O'Neill, and B. Richter, Phys. Rev. Letters **16**, 1127 (1966), and more recent data reported by G. K. O'Neill at the Fourteenth International Conference on High Energy Physics, Vienna, Austria 1968 (unpublished) (spacelike photons).

²The other dominant amplitude involves a spacelike electron: $q_s^2 = (p_1 - k)^2 < 0$. The two amplitudes are comparable, but since only the sum is gauge invariant, their relative importance depends on the gauge chosen for the calculation. One can vary q_t^2 and q_s^2 independently, however.

³In contrast to the situation in the wide-angle pair production experiments, there is no advantage in having $\theta_2 = \theta_\gamma$.

⁴Preliminary results of this experiment, based on a smaller data sample, were reported at the Fourteenth International Conference on High Energy Physics, Vienna, Austria, 1968 (unpublished). Also reported were the results of another wide-angle bremsstrahlung experiment at lower energies: C. Bernardini, F. Felicetti, L. Meneghetti-Vitale, G. Penso, R. Querzoli, V. Silvestrini, G. Vignola, and S. Vitale, Laboratori Nazionali di Frascati Report No. LNF-68/46 (unpublished).

⁵R. R. Wilson, Nucl. Instr. **1**, 101 (1957). The quantummeter calibration has been checked by comparison with a Faraday cup: R. Gomez, J. Pine, and A. Silverman, Nucl. Instr. **24**, 429 (1963).

⁶The exact cross section was used in the analysis of the data: H. A. Bethe and W. Heitler, Proc. Roy. Soc. (London), Ser. A **143**, 83 (1934). For a modern derivation see R. P. Feynman, Quantum Electrodynamics (W. A. Benjamin, Inc., New York, 1961), p. 107 (the angle φ is incorrectly shown in Fig. 22-1).

⁷The elastic carbon form factor was taken from the data of J. H. Fregeau, Phys. Rev. **104**, 225 (1956). Inelastic effects (less than 5%) were estimated following the methods of S. D. Drell and C. L. Schwartz, Phys.

Rev. **112**, 568 (1958), and W. L. Faissler, F. M. Pipkin, and K. C. Stanfield, Phys. Rev. Letters **19**, 1202 (1967).

⁸Including a 2% correction for bremsstrahlung by the incident or recoil electron elsewhere in the target along the flight path in the spectrometer.

⁹For a discussion of possible modifications of quantum electrodynamics see N. M. Kroll, Nuovo Cimento **45A**, 65 (1966). A model which would predict a spectacular deviation from conventional quantum electrodynamics for timelike electrons has been suggested by F. E. Low, Phys. Rev. Letters **14**, 238 (1965).

BREAKDOWN OF THE VECTOR DOMINANCE RELATION BETWEEN ρ^0, ω PRODUCTION AND POLARIZED PHOTOPRODUCTION*

L. J. Gutay, F. T. Meiere, J. H. Scharenguivel, D. H. Miller,
R. J. Miller, S. Lichtman, and R. B. Willmann

Purdue University, Lafayette, Indiana 47907

(Received 8 January 1969)

The validity of vector-meson dominance is tested by comparing our high statistics ρ^0 and ω production experiments at 2.7 and 4 GeV/c with the results of polarized photopion production experiments. Our results suggest the breakdown of the vector-dominance model even after taking into account the strong S -wave $\pi\pi$ interaction in the ρ^0 region.

It was suggested by Gell-Mann and Zachariasen¹ that the hadronic electromagnetic currents are dominated by the vector mesons ρ , ω , and φ . (Hereafter the vector-meson-dominance assumption will be abbreviated by VMD.) Although this model has a wide range of applicability, we restrict our attention to the study of certain aspects of the reactions

$$\pi^- p \rightarrow \pi^+ \pi^- n, \quad (1a)$$

$$\pi^+ d \rightarrow \pi^+ \pi^- p p_s, \quad (1b)$$

$$\pi^+ d \rightarrow \pi^+ \pi^- \pi^0 p p_s \quad (1c)$$

observed in bubble chambers.^{2,3} Our results on Reactions (1) are compared with those of a counter experiment of Geweniger *et al.*⁴ who studied the reactions

$$\gamma n \rightarrow \pi^- p, \quad (2a)$$

$$\gamma p \rightarrow \pi^+ n, \quad (2b)$$

where the incident photon was linearly polarized. Their results gave the first indication of the breakdown of VMD. Our comparison supports this conclusion.

We have analyzed 4477 events of Reaction (1a) and 3256 events of Reaction (1b) both at 2.7 GeV/c. The production and decay angular distributions of the di-pion system agreed within errors and the data from Reactions (1a) and (1b) were

combined and used as a single sample in the following analysis. In addition we analyzed 3348 events of Reaction (1c) at 2.7 GeV/c and 7916 events of Reaction (1a) at 4 GeV/c. The 4-GeV/c data are the result of the Purdue-Notre Dame-Stanford Linear Accelerator Center-Lawrence Radiation Laboratory Collaboration.³ The density matrix elements for ω production (1c) at 3.65 GeV/c were taken from Benson.⁵

The photoproduction experiment of Geweniger *et al.*⁴ was done with an incident photon energy of 3.4 GeV. Thus the center-of-mass system energy for the photoproduction reactions (2) is bracketed by our data on vector-meson production.

By VMD we mean the assumption that the photoproduction amplitude is related to the amplitude for production of transverse vector mesons by⁶

$$\langle \pi N | T | \gamma N \rangle = \sum g_V \langle \pi N | T | V N \rangle, \quad (3)$$

where g_V are the known photon-vector-meson coupling constants. We keep only the ρ^0 and ω contribution to Eq. (3). The φ contribution is negligible.⁷ The $\rho^0\omega$ interference terms are eliminated by considering the following sum of cross sections:

$$\frac{d\sigma}{dt} = \frac{d\sigma}{dt}(\gamma p \rightarrow \pi^+ n) + \frac{d\sigma}{dt}(\gamma n \rightarrow \pi^- p). \quad (4)$$

The ρ^0 contribution is determined by the differential cross section for the reaction $\pi N \rightarrow \pi\pi N$ which is given by⁸

$$\frac{\partial^4 \sigma}{\partial s \partial \Delta^2 \partial \theta \cos \theta \partial \phi} = \frac{1}{4\pi} \{ R_{00}^{00} + 2R_{11}^{11} + R_{00}^{11} + (R_{00}^{11} - R_{11}^{11})(3 \cos^2 \theta - 1) - 3\sqrt{2} \operatorname{Re}(R_{10}^{11}) \sin 2\theta \cos \phi - 3R_{1-1}^{11} \sin^2 \theta \cos 2\phi - 2\sqrt{6} \operatorname{Re}R_{10}^{10} \sin \theta \cos \phi + 2\sqrt{3}R_{00}^{10} \cos \theta \}, \quad (5)$$